A Comparative Study of CNN Architectures for Melanoma Skin Cancer Classification

Khadidja Belattar[1][0000−0003−4101−7135], Maya Adjadj[1], Maya Bakir[1], and Mohamed Ait Mehdi[2][0000−0002−6225−4642]

[1] University of Algiers, Algiers, Algeria
[2] LRIA, USTHB, Algiers, Algeria
khadidja.belattar@gmail.com
maitmehdi@usthb.dz

Abstract. Skin cancer is recognized as one of the common and deadliest cancer. Therefore, an easy, early and discriminatory diagnosis of the skin cancer would be crucial to ensure appropriate and effective treatment for patients. Although there are many computerized methods for classifying skin lesions, Convolutional Neural Networks (CNN) have proven superior to the conventional methods.
In the present work, we investigated seven deep neural network classifiers, namely, baseline CNN, InceptionV3, ResNet50, VGG16, Xception, MobileNetV2 and DenseNet201 to predict the input skin lesion class (melanoma or nevus). The adapted architectures were tested on 1500 ISIC images and the comparisons of the obtained results with the EfficientNetB3 as well as InceptionResNetV2 have demontrated the superiority of the Baseline CNN, DenseNet201 and Xception. These models would provide a strong automated support for the melanoma diagnosis and could be exploited in the classification of eczema and psoriasis skin lesions.

Keywords: Melanoma diagnosis · CNN · InceptionV3 · ResNet50 · VGG16· Xception · MobileNetV2 · DenseNet201 · EfficientNetB3 · InceptionResNetV2.

1 Introduction

Medical image recognition is a fundamental task in medical image analysis applications. Generally speaking, it refers to the process of the identification of the objects of interest and the diagnosis of the disease within medical images [1]. In principle, the medical image recognition is used to assist the medical professionals in the interpretation of medical images with the aid of the automatic tools. The importance of fast and reliable diagnostic tools has been brought to the fore with the COVID-19 pandemic. Indeed, the image recognition systems are beginning to find a foothold in prime medical applications including COVID-19 recognition [2], ophthalmic disease detection [3], pneumonia detection [4], malaria parasite detection [5], Alzheimer's disease detection [6], breast

cancer detection [7], tuberculosis disease diagnosis [8], colon cancer classification [9], and the skin lesion diagnosis [10]. In this respect, there exists a variety of medical diagnostic methods [11]. The leading ones include the physical and visual examination, cellular and chemical analysis, genetic testing and imaging methods.

Dermatoses are among the four most common health concerns in ill patients. Skin cancer, most particularly melanoma, represents a serious and deadly form of the skin cancer, in which there is an abnormal growth of melanocyte skin cells. The early signs of melanoma are usually changes in the shape, color (usually pigmented), size, texture or bleeds of the skin over time. In the advanced stage, the melanoma cells have spread, or metastasize, throughout the body. Hence, the survival rate declines with later stages of the melanoma. Fortunately, an early and reliable diagnosis of the skin cancer could greatly increase a patient's chance of successful treatment and enhance the survival rate. However, diagnosing the melanoma timely and accurately is a challenging task. This is due to several reasons. Firstly, different artifacts, such as the hair strands, could occlude the skin lesion. Secondly, the high intra-class variations of the skin lesion which means that the treated melanoma is manifested with a diverse visual features including: the lesion color, the shape, the size, the location, the structure and distribution. Moreover, the melanoma skin lesions can closely resemble the non-cancer skin lesions. Indeed, different skin lesion kinds can have similar clinical features (i.e the high inter-class similarity), furthering the problem in discriminating among them. And the last reason, the diagnosis of the melanoma heavily depends on the experience of dermatologists and requires time [12]. Therefore, a Computer-Aided Diagnosis (CAD) system would be useful screening tool to reach an enhanced diagnosis quality as soon as possible. Generally speaking, the CAD system in the dermatological imaging is the computerized analysis of the dermatological images to recognize the required skin lesion. Most of the CAD techniques can be conventional skin lesion image classification, or based on computer vision algorithms. The conventional methods for the skin lesion diagnosis [13–15] are labor-intensive and typically depend on the predefined handcrafted features with respect to a specific skin disease diagnosis task. So, the CAD system can recognize well a particular skin disease. However, it is unable to be generalized on broader classes of the skin diseases for the diagnosis purposes [16]. This is due to the complexity and the diversity of the skin diseases. So, the feature learning [17] could be an interesting solution to the stated problem. The idea is to learn automatically the high-level image features from the input raw data without the need of the feature engineering process. In the context of the skin lesion diagnosis, various feature learning approaches have been presented in the literature [18–21]. Recently, deep learning algorithms have made a significant advances in the feature learning topic and provide superior performances in various tasks, including the image classification [22], image segmentation [23,24] and object detection [25].

Our goal, in this work, is to establish a consistent comparative study of the performance of the most common deep learning models for the melanoma

diagnosis purposes. The achieved findings could be explored in the future for other skin diseases or medical analysis tasks.

The structure of the paper is as follows. Section 2 presents the recent state of the art in the context of skin lesion diagnosis based on deep learning models. In Section 3, we investigate seven common deep learning models for the melanoma diagnosis purposes on ISIC image database. Section 4 addresses the experimental results and discussion of the most important findings of the performed comparative study. Finally, Section 5 concludes the research work.

2 Literature Review

Deep neural network architectures have recently emerged and developed to solve different problems in particular the skin lesion diagnosis. The research literature has progressed towards basic convolutional neural network, transfer learning-based CNN architectures, ensemble learning and transformers.

In the last few years, a significant number of research papers has been published on the topic of the skin lesion diagnosis. In particular, Li et al. (2021) [26] published a recent review article that summarized the existing deep learning-based skin disease segmentation and diagnosis methods undertaken between 2015 and 2019. However, the latest studies in the field were not incorporated in this work. Therefore, in this section, we established an overview of the most recent deep learning approaches for the pigmented skin lesion classification.

Hosny et al. (2020) [27] established the classification of the skin lesions into seven classes based on AlexNet architecture. The proposed method was tested using the dataset ISIC 2018. The achieved percentages are 98.70%, 95.60%, 99.27%, and 95.06% for accuracy, sensitivity, specificity, and precision, respectively.

While in [28], Al-Masni et al. (2020) suggested multiple skin lesions diagnostics framework. The latter combines the skin lesion segmentation and classification processes. Firstly, the authors attempted to segment the skin lesion from dermoscopic images by employing a full resolution CNN architecture. Then, four CNN classifiers were used, namely : Inception-v3, ResNet-50, Inception-ResNet-v2, and DenseNet-201, to discriminate between different skin diseases. The proposed framework is evaluated using ISIC 2016, ISIC2017 and ISIC 2018. The Inception-v3, ResNet-50, Inception-ResNet-v2, and DenseNet-201 models give the overall weighted prediction accuracies of 88.05%, 89.28%, 87.74%, and 88.70% for seven classes of ISIC 2018, respectively.

An automatic classification system of the skin lesion images is developed by Samanta and Rout (2021) [29]. In the developed system, the VGGNet architecture is applied to classify the ISIC skin lesions as malignant or benign. The used model achieves a classification accuracy rate of 98.02%, the sensitivity of 98.10%, and specificity of 97.05%.

Another research proposed by Sikkandar et al. (2021) [30]. The authors presented a skin lesion segmentation method-based classification model for skin lesion diagnosis. The method is based on four steps, namely : the skin lesion image preprocessing, segmentation, feature extraction and classification. The authors

first introduced top hat filter and inpainting technique, followed by the application of the GrabCut algorithm. Then, the feature extraction stage involves the use of a deep learning-based Inception model. In the last step, an adaptive neuro-fuzzy model is used to classify the dermoscopic images into different classes.

Miglani and Bhatia (2021) [31] established the EfficientNet family of models to the skin classification task in comparison with the ResNet architecture. To test and evaluate the adapted model performance, the authors used a dataset comprising 10015 dermatoscopic images belonging to seven classes of the skin cancer. Hence, EfficientNet-B0 algorithm is able to classify the skin lesion with macro and micro average ROC AUC of 0.93 and 0.97, respectively.

A CNN-based deep learning framework has been developed by Özbay and Özbay (2021) [32]. The authors proposed forty five layers-based CNN model for the cancer diagnosis from dermatoscopic skin lesion images. Regarding the performance evaluation of the model, a HAM10000 dataset has been used which includes 10015 dermatoscopic images in total. An accuracy value of 99.69% is obtained with the model developed for the classification of cancer image.

Ali et al. (2021) [33] designed a deep convolutional neural network model that classifies the skin cancer in three steps. The authors firstly, applied a mean filter to remove the noise and artifacts from the input image, besides the image normalization. Secondly, a set of features are extracted and data augmentation techniques are used. At last, CNN-based classification step is performed. The model is evaluated on the HAM10000 dataset and it achieves the highest 93.16% of training and 91.93% of testing accuracy, respectively.

Bansal et al. (2022) [34] introduced an intelligent system for the detection of the melanoma from dermoscopic images. First, the authors used various morphological operations for the hair removal task. In the feature extraction stage, a combined features are computed from the handcrafted feature extraction techniques and deep learning models (ResNet50V2 and EfficientNet-B0). As a final stage, the authors used a neural network model for the classification. The proposed system has been validated on two datasets : HAM10000 consisting of 10015 dermoscopic images belonging to seven classes and PH2 dataset of 200 melanoma and non melanoma dermoscopic images. An accuracy of 94.9% and 98% is achieved on HAM10000 and PH2 datasets, respectively.

A more recent work was carried out by Salma and Eltrass (2022) [35] to develop a new computer-aided diagnosis system for the skin lesion classification. The authors employed the morphological filtering to remove different artifacts. Then, the skin lesions are segmented automatically using the GrabCut in HSV color space. After that, the ABCD (asymmetry, border irregularity, color and dermoscopic patterns) rule is implemented to extract the relevant features. Finally, the resulted ABCD features are feed into different pretrained CNN architectures, including VGG-16, ResNet50, ResNetX, InceptionV3, and MobileNet, to classify the skin lesions into benign or malignant skin lesions. Furthermore, the proposed classification system is improved by integrating the kernel SVM classifier with the used CNN architectures. The ResNet50 architecture combined with

the SVM model achieves area under the ROC curve (ROC-AUC) of 99.52%, accuracy of 99.87%, sensitivity of 98.87%, precision of 98.77% and F1-score of 97.83%.

The skin lesion classification problem could be also solved using ensemble learning-based methods, the commonest ones are : combination of the CNN and One-versus-All [36], ensemble of EfficientNets, SENet and ResNeXt WSL [37], triplet-based CNN [38], AlexNet and GoogLeNet [39].

Based on the above mentioned literature review, several CNN model-based publications are demonstrated in the field of the computer-aided melanoma diagnosis, since they provide promising image classification results and do not require more computing power in model training as well as in classification compared to the recurrent neural networks and reinforcement learning models. Our aim is to facilitate and enhance the skin cancer diagnosis. So, we take advantage of the most common and successful CNN models to perform the present comparative study. Such an investigation undertaken in the melanoma diagnosis field has been missing. In this work, we focus on performance comparison of seven CNN architectures for melanoma classification, namely : baseline CNN, InceptionV3, ResNet50, VGG16, Xception, MobileNetV2 and DenseNet201.

3 Materials and Models

This section provides a description of the material and models we have employed to develop the proposed diagnosis system. It is organized in four subsections, namely : dataset, CNN architectures, tuning hyperparameters settings and the performance evaluation.

Technically speaking, the adapted CNN architectures were implemented using Python programming language and were trained as well as tested on Google Colaboratory (usually referred to as Colab) platform with a 12.8 GB of Ram and a free GPU.

3.1 Dataset

The melanoma differential diagnosis process first requires using datasets. In this study, we used ISIC 2019 dataset. It consists of 25,331 dermoscopic labelled images, belonging to nine types of skin lesions. From the whole dataset, we used only two basic classes; melanoma and nevus skin lesions. However, the used dataset is imbalanced, so, we constructed a balanced dataset by selecting 765 melanoma and 765 nevus images of the high quality. So, we focused on artifact-free images to ensure better generalization of the adapted models. The total number of the used images to undertake the study was limited to the used resources. Once the dataset is created, we prepared the skin lesion images for the melanoma classification process through:

Data Preprocessing Data preprocessing task involves two main steps. We first resize the used skin lesion images to have the same input size as the adapted

CNN architectures. Then, we apply the input normalization of the resized skin lesion images.

Dataset Sampling Splitting data into train, test, and validation sets is a common task in machine learning. In this stage, we used the following proportions : 70% training, 15% validation, and 15% testing in which each set has equal proportion of melanoma and nevus images. Table 1 illustrates the distribution of data samples among different classes in training, validation and test partitions.

Table 1. Melanoma image distribution in training, validation and test sets

	Melanoma	Nevus	Total
Training set	525	525	1050
Validation set	120	120	240
Test set	120	120	240

The three obtained data sets are commonly exploited in the training and classification stages of the adapted CNN architectures.

3.2 CNN Architectures : Training and Classification

Among all the reviewed CNN architectures, we employed the baseline CNN and pretrained architectures as these models are popular and showed remarkable performance. For all pretrained architectures, the transfer learning is involved. Also, we used the cross-entropy loss function during the training stage.

- Baseline CNN : consists of the first input layer, three convolutional and pooling layers, followed by the fully connected layer with the drop out regularization. The classification is done via the last fully connected layer.
- InceptionV3 [40] : is the arrangement of the stem block, three inception modules (A, B, C), two reduction blocks (A, B) and classification block. The stem block contains a concatenation of multiple convolutional and pooling layers while the inception modules are composed of a set of convolutional filters with an average pooling layer. In the reduction blocks, the max pooling operation is applied. The final classification block includes the global max pooling layer with the batch normalization and two fully connected layers. The skin lesion classification is enhanced by applying the drop out regularization after each a fully connected layer and inserting the final fully connected layer.
- ResNet50 [41] : has sixteen residual blocks. It incorporates two kinds of shortcut module, namely : identity and convolution blocks. The identity block is defined as three convolution layers in the main path and no convolution layer at shortcut. The convolution block has the convolution layer at shortcut path and three convolution layers in the main path. The output of the final residual block is flatten, then three fully connected layers are used.

- VGG16 [42] : comprises of thirteen convolution layers of 3x3 filter and five max pooling layers of 2x2 filter. These layers generate the image feature map which is flatten with the batch normalization in the skin lesion classification layers. Next, the fully connected layer with the batch normalization is inserted, followed by one lambda layer and the VGG 16 architecture ends with the last fully connected layer.
- Xception [43]: is a network that involves stacking the depthwise separable convolution layers with the residual connections. The next layers are made up of the global max pooling layer and fully connected layer. We applied for both layers the batch normalization technique. After that, the drop out regularization is applied followed by one fully connected layer with the batch normalization. In the end, another fully connected layer with the drop out regularization is added for the skin lesion classification.
- MobileNetV2 [44]: includes the convolutional layer, followed by seventeen residual bottleneck blocks. Each one has three layers : convolution layer with a rectified linear unit, depthwise convolution, and another convolution layer without non-linearity. These blocks are succeeded by a single convolution layer, with the max pooling layer. Further batch normalization operations, fully connected layers and drop out regularization are incorporated with the MobileNetV2 architecture. The last layer is the fully connected classification.
- DenseNet201 [45]: is composed of four Dense blocks. In each dense block, two convolution operations are applied; with 1x1 and 3x3 sized kernels. The DenseNet201 architecture begins with the main convolution and pooling layers. After that, the dense blocks are introduced. The first three dense blocks are followed by the transition layer meanwile the last one is followed by an average pooling layer. For the skin lesion classification, two fully connected layers with the batch normalization and drop out regularization operations are added followed by the final fully connected layer.

Table 2 presents the number of layers and number of parameters of the trained models.

Table 2. An overview of the trained CNN models for the melanoma classification

CNN architecture	Number of layers	Number of parameters
Baseline CNN	**11**	7.4 M
InceptionV3	315	23,9 M
ResNet50	180	25.6 M
VGG16	25	138.4 M
Xception	141	22.9 M
MobileNet V2	158	**3.5 M**
DenseNet 201	716	20.2 M

3.3 Tuning Hyperparameters Settings

The hyperparameters tuning plays a significant role in the deep neural netwok prediction process. Our goal is to select the optimal combination of hyperparameters so that the model can have an improved classification ability. In this study, we trained the seven adapted CNN models several times with different values of the hyperparameters to get the best classification results. The settings shown on table 3 have been adopted.

Table 3. Hyperparameters fine-tuning of the CNN models

Hyper parameter	Value
Batch size	50
Epochs	[15 - 35]
Activation functions	RelU, Softmax
Optimizer	Adam
Learning rate	0.0001
Dropout rate	[0.4 - 0.8]

3.4 Performance Evaluation

To check the CNN model performance, we used the most common measures, namely : the accuracy, precision, recall (sensitivity) and specificity of the melanoma classification. These measures are given as follows :

$$Accuracy = \frac{TP + TN}{TP + TN + FP + FN} \tag{1}$$

$$Precision = \frac{TP}{TP + FP} \tag{2}$$

$$Recall = \frac{TP}{TP + FN} \tag{3}$$

$$Specificity = \frac{TN}{TN + FP} \tag{4}$$

Where: TP (True Positive) is the number of accurately labeled positive samples, TN (True Negative) is the correctly classified negative samples, FP (False Positive) is the number of negative examples classified as positive, and FN (False Negative) is the number of positive samples predicted as negative.

4 Melanoma Classfication Results

In this section, we report the results of the experimental evaluation of the seven CNN architectures (baseline CNN, InceptionV3, ResNet50, VGG16, Xception, MobileNetV2 and DenseNet201) for the melanoma diagnosis.
Fig 1 a illustrates the accuracy performance of seven CNN models for the melanoma classification.

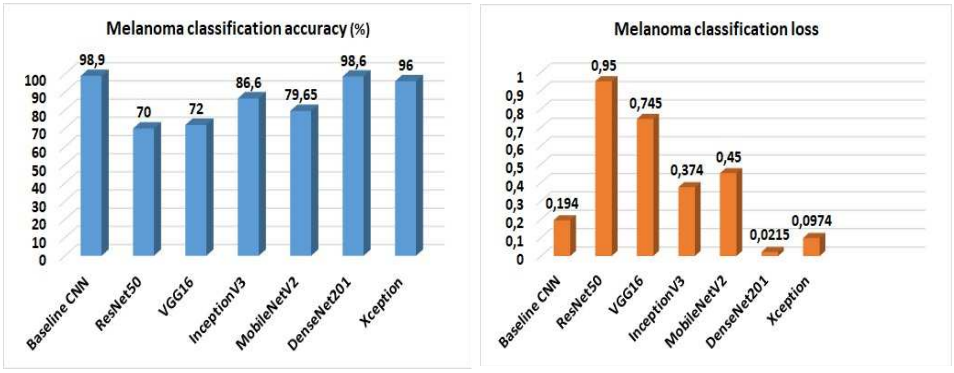

(a) Accuracy (b) Loss

Fig. 1. Classification performance of the adapted models

Among all the used models, Simple CNN and DenseNet201 provide the highest classification accuracy of around 98%. The Xception also shows considerable performance and contribute an accuracy of 96%. The InceptionV3 records a reasonable accuracy of around 86.6% while MobileNetV2 achieves an accuracy of 79.65%. However, VGG16 and ResNet50 produce the lowest accuracy of around 70%.
We also computed the classification loss of the above mentioned models, as shown in the Fig 1 b. It is perceived from the figure, the best loss value for the classification is attained by DenseNet201, followed by Xception with a value of 0.0974. The baseline CNN attains the loss value of 0.194. On the other hand, InceptionV3 and MobileNetV2 deliver the loss values of 0.374 and 0.45, respectively whereas VGG16 and RestNet50 show the least performance.

As Baseline CNN, DenseNet201 and Xception achieve a remarkable compromise between the model complexity (expressed by the number of parameters), the accuracy and loss compared to that of the other architectures, we present, in the Fig 2, table 4 and table 5 the obtained results. Accordingly, the Fig 2 illustrates the accuracy and loss curves of these models for the training and validation sets. We observe that the Xception has more stable curves than those of the Baseline CNN and DenseNet201. The latter delivers the best accuracy

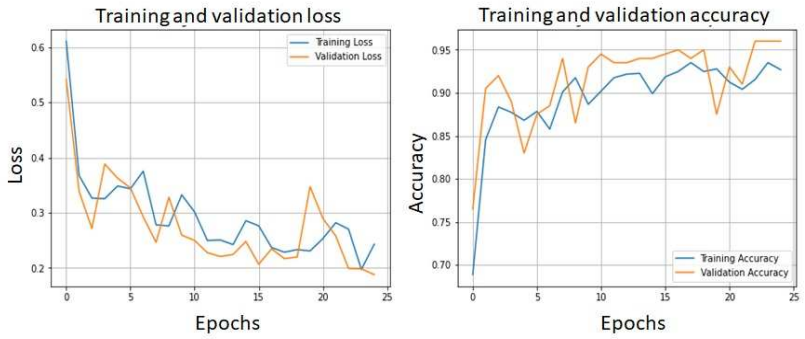

(a) Baseline CNN

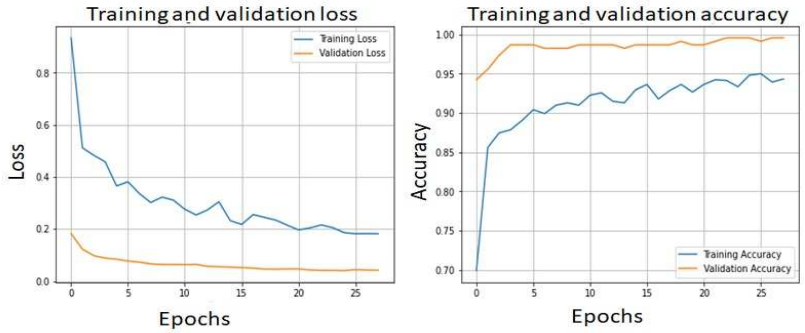

(b) DenseNet201

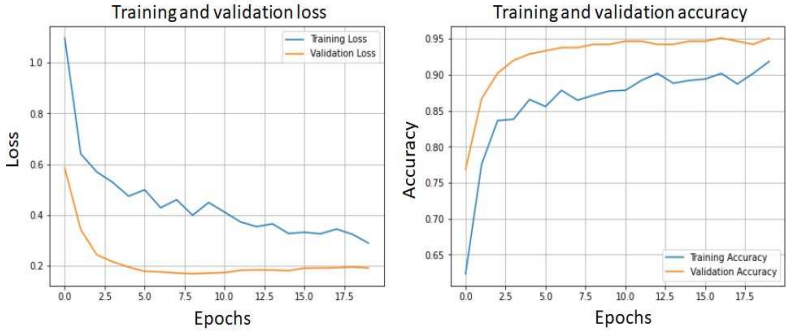

(c) Xception

Fig. 2. Loss and accuracy curves of the best CNN architectures

and loss values for the training and validation sets. The accuracy plots of the trained data for both the networks are rising quickly to around 84% from epoch 0 to 2. The Baseline CNN converges to a value of over 93.02% after epoch 25, the DenseNet201 converges to a value of 94.31% while Xception converges to a value of 91.8%. Similarly, the validation accuracy reached during the model

validation is around 96.88% for the Baseline CNN, 99.5% for the DenseNet201 and 95.1% for the Xception architecture. Regarding the loss curve of the training and validation data, the Basline CNN loss is fluctuating considerably and it produces the training and validation loss of about 0.21 and 0.19, respectively, after 25 epochs. However, if we perceive the loss curves of the DenseNet201, it is regarded that the training loss dropped to 0.39 within the first five epochs and reaches a relatively stable value of about 0.18 from 23 th epochs. Moreover, the loss curve of validation data converges to a value of 0.0417. For the Xception, the model yields the training and validation loss of about 0.29 and 0.19, respectively. To show the classification performance of the Baseline CNN, DenseNet201 and Xception, table 4 depicts the TP, TN, FP and FN values, computed from the confusion matrices on the test set. As we notice from the table, the Baseline CNN

Table 4. TP, TN, FP, and FN results of the Baseline CNN, DenseNet201 and Xception models

Model	TP	TN	FP	FN
Baseline CNN	**118**	**119**	**1**	**2**
DenseNet201	117	118	2	3
Xception	114	117	3	6

attains the highest classification accuracy compared to those of the DenseNet201 and Xception. It is also perceived that the Baseline CNN (DenseNet201, Xception) can accurately recognize 118 (117, 114, respectively) images in the melanoma class, though two (three, six, respectively) images are labeled as nevus class. Besides, in the nevus image class, 119 (118, 117, respectively) images are identified precisely but, one (two, three, respectively) image(s) is(are) listed in the melanoma class.
Table 5 shows the precision and recall performance of the used architectures for the melanoma classification. In overall, the three CNN models perform well in the precision and recall measures for the nevus and melanoma classes.

Table 5. Precision and recall evaluation of the Baseline CNN, DenseNet201 and Xception models

Architecture	Class	Precision (%)	Recall (%)
Baseline CNN	Nevus	98	**99**
	Melanoma	**99**	**98**
DenseNet201	Nevus	98	98
	Melanoma	98	97
Xception	Nevus	96	95
	Melanoma	96	97

4.1 Analysis and Discussion

Generally speaking, CNN-based image classification system performance is affected by the imaging modality, image quality, image content, dataset size, distribution of the image classes, number of classes, the architecture of the model (number of layers and number of neurons), the model complexity, the hyperparameters configurations and the use of the regularization methods.

As shown in the obtained results, the Baseline CNN, DenseNet201 and Xception perform well compared to the InceptionV3, ResNet50, VGG16 and MobileNetV2. Therefore, the results demonstrate that the lightweight architectures (with reduced number of parameters) give better classification accuracy, loss, average precision, average recall and ROC-AUC values in this type of image dataset. Such architectures employ the skip connections and as all we know, these connections reduce the number of parameters while dealing with the vanishing gradient problem. Therefore, the classification results are enhanced.
If we analyze the architecture of the Baseline CNN, it is noticed that it has shallow network, simple and straightforward architecture compared to all other models. We also see that though the considerable network depth of the DenseNet201, it could give better classification performance than those of the shallow networks (such as InceptionV3 and ResNet50). Furthermore, the number of parameters of the DenseNet201 model is two times more than that of the MobileNetV2. Inspite of this, the DenseNet201 provides better results than those of the MobileNetV2. This is may be due to the effectiveness of the feature map generation method of the dense blocks. The batch normalization and drop out regularization could be another reason behind the improved performance of the lightweight architectures.

4.2 Models Comparison

Related comparisons have been presented in this subsection. So, we implemented the InceptionResNetV2 [28] and EfficientNetB3 [31], using the same hepyerparameters settings. They are compared to the Baseline CNN, DenseNet201 and Xception architectures, as shown in Table 6.
It is clear that the Baseline CNN, DenseNet201 and Xception models outperform the EfficientNetB3 and InceptionResNetV2 in terms of the accuracy (Acc), loss, average precision (AP), average recall (AR) and $AUCscore$.

Table 6. Comparison of CNN archietctures

Model	$Acc(\%)$	$Loss$	$AP(\%)$	$AR(\%)$	$AUCscore$
Baseline CNN	**98.9**	0.19	**98.5**	**98.5**	**0.99**
DenseNet201	98.6	**0.0215**	98	97.5	0.98
Xception	96	0.097	96	96	0.96
InceptionResNetV2	80	0.4	54	53	0.53
EfficientNetB3	78	0.87	79	78	0.78

5 Conclusion and Perspectives

In this paper, we present a comparative study of seven CNN architectures for the computer-aided melanoma diagnosis. The adapted models improved the classification performance, but the outcomes show that the Baseline CNN, DenseNet and Xception have much better performance.

In future, we will consider a large skin lesion image dataset with more classes. Further work will focus on designing an ensemble model to enhance the classification performance as well as extending the CNN architectures to different kinds of skin lesions such as eczema and psoriasis. Another interesting direction would be to explore more advanced deep learning models for the skin lesion diagnosis.

References

1. Zhou, S.K.: Introduction to medical image recognition, segmentation, and parsing. In: Medical Image Recognition, Segmentation and Parsing, pp. 1–21. Elsevier (2016)
2. Altan, A., Karasu, S.: Recognition of covid-19 disease from x-ray images by hybrid model consisting of 2d curvelet transform, chaotic salp swarm algorithm and deep learning technique. Chaos, Solitons & Fractals 140, 110071 (2020)
3. Sengupta, S., Singh, A., Leopold, H.A., Gulati, T., Lakshminarayanan, V.: Ophthalmic diagnosis using deep learning with fundus images–a critical review. Artificial Intelligence in Medicine 102, 101758 (2020)
4. Ortiz-Toro, C., García-Pedrero, A., Lillo-Saavedra, M., Gonzalo-Martín, C.: Automatic detection of pneumonia in chest x-ray images using textural features. Computers in Biology and Medicine 145, 105466 (2022)
5. Lee, Y.W., Choi, J.W., Shin, E.H.: Machine learning model for predicting malaria using clinical information. Computers in Biology and Medicine 129, 104151 (2021)
6. Singh, A., Kharkar, N., Priyanka, P., Parvartikar, S.: Alzheimer's disease detection using deep learning-cnn. In: Ambient Communications and Computer Systems, pp. 529–537. Springer (2022)
7. Ravikumar, M., Rachana, P.: Study on different approaches for breast cancer detection: A review. SN Computer Science 3(1), 1–6 (2022)
8. Oltu, B., Güney, S., Dengiz, B., Ağıldere, M.: Automated tuberculosis detection using pre-trained cnn and svm. In: 2021 44th International Conference on Telecommunications and Signal Processing (TSP). pp. 92–95. IEEE (2021)
9. Aurelia, J.E., Rustam, Z., Wibowo, V.V.P., Setiawan, Q.S.: Comparison between convolutional neural network and convolutional neural network-support vector machines as the classifier for colon cancer. In: 2020 International Conference on Decision Aid Sciences and Application (DASA). pp. 812–816. IEEE (2020)
10. Li, H., Pan, Y., Zhao, J., Zhang, L.: Skin disease diagnosis with deep learning: a review. Neurocomputing 464, 364–393 (2021)
11. Korbicz, J., Kowal, M.: Intelligent systems in technical and medical diagnostics. Springer (2014)
12. Morton, C., Mackie, R.: Clinical accuracy of the diagnosis of cutaneous malignant melanoma. The British journal of dermatology 138(2), 283–287 (1998)
13. Arroyo, J.L.G., Zapirain, B.G.: Automated detection of melanoma in dermoscopic images. In: Computer vision techniques for the diagnosis of skin cancer, pp. 139–192. Springer (2014)

14. Saez, A., Acha, B., Serrano, C.: Pattern analysis in dermoscopic images. In: Computer vision techniques for the diagnosis of skin Cancer, pp. 23–48. Springer (2014)
15. Madooei, A., Drew, M.S.: Incorporating colour information for computer-aided diagnosis of melanoma from dermoscopy images: A retrospective survey and critical analysis. International journal of biomedical imaging 2016 (2016)
16. Habif, T.P., Chapman, M.S., Dinulos, J.G., Zug, K.A.: Skin disease e-book: diagnosis and treatment. Elsevier Health Sciences (2017)
17. Bengio, Y., Courville, A., Vincent, P.: Representation learning: A review and new perspectives. IEEE transactions on pattern analysis and machine intelligence 35(8), 1798–1828 (2013)
18. Cruz-Roa, A.A., Arevalo Ovalle, J.E., Madabhushi, A., González Osorio, F.A.: A deep learning architecture for image representation, visual interpretability and automated basal-cell carcinoma cancer detection. In: International conference on medical image computing and computer-assisted intervention. pp. 403–410. Springer (2013)
19. Jadhav, A.R., Ghontale, A.G., Shrivastava, V.K.: Segmentation and border detection of melanoma lesions using convolutional neural network and svm. In: Computational Intelligence: Theories, Applications and Future Directions-Volume I, pp. 97–108. Springer (2019)
20. Benyahia, S., Meftah, B., Lézoray, O.: Multi-features extraction based on deep learning for skin lesion classification. Tissue and Cell 74, 1–24 (2022)
21. Deepika, P.A., Yamini, B.: Classification of skin lesions using svm via deep learning feature network. Advanced Science and Technology 29, 4526–4538 (2020)
22. Krizhevsky, A., Sutskever, I., Hinton, G.E.: Imagenet classification with deep convolutional neural networks. Advances in neural information processing systems 25 (2012)
23. Badrinarayanan, V., Kendall, A., Cipolla, R.: Segnet: A deep convolutional encoder-decoder architecture for image segmentation. IEEE transactions on pattern analysis and machine intelligence 39(12), 2481–2495 (2017)
24. Chen, L.C., Papandreou, G., Kokkinos, I., Murphy, K., Yuille, A.L.: Deeplab: Semantic image segmentation with deep convolutional nets, atrous convolution, and fully connected crfs. IEEE transactions on pattern analysis and machine intelligence 40(4), 834–848 (2017)
25. Pathak, A.R., Pandey, M., Rautaray, S.: Application of deep learning for object detection. Procedia computer science 132, 1706–1717 (2018)
26. Li, H., Pan, Y., Zhao, J., Zhang, L.: Skin disease diagnosis with deep learning: a review. Neurocomputing 464, 364–393 (2021)
27. Hosny, K.M., Kassem, M.A., Fouad, M.M.: Classification of skin lesions into seven classes using transfer learning with alexnet. Journal of digital imaging 33(5), 1325–1334 (2020)
28. Al-Masni, M.A., Kim, D.H., Kim, T.S.: Multiple skin lesions diagnostics via integrated deep convolutional networks for segmentation and classification. Computer methods and programs in biomedicine 190, 105351 (2020)
29. Samanta, P.K., Rout, N.K.: Skin lesion classification using deep convolutional neural network and transfer learning approach. In: Advances in Smart Communication Technology and Information Processing, pp. 327–335. Springer (2021)
30. Sikkandar, M.Y., Bader, A.A., Prakash, N., Hemalakshmi, G., Mohanarathinam, A., Shankar, K.: Deep learning based an automated skin lesion segmentation and intelligent classification model. Journal of ambient intelligence and humanized computing 12(3), 3245–3255 (2021)

31. Miglani, V., Bhatia, M.: Skin lesion classification: A transfer learning approach using efficientnets. In: International Conference on Advanced Machine Learning Technologies and Applications. pp. 315–324. Springer (2020)
32. Özbay, E., Özbay, F.A.: A cnn framework for classification of melanoma and benign lesions on dermatoscopic skin images. International Journal of Advanced Networking and Applications 13(2), 4874–4883 (2021)
33. Ali, M.S., Miah, M.S., Haque, J., Rahman, M.M., Islam, M.K.: An enhanced technique of skin cancer classification using deep convolutional neural network with transfer learning models. Machine Learning with Applications 5, 100036 (2021)
34. Bansal, P., Garg, R., Soni, P.: Detection of melanoma in dermoscopic images by integrating features extracted using handcrafted and deep learning models. Computers & Industrial Engineering 168, 108060 (2022)
35. Salma, W., Eltrass, A.S.: Automated deep learning approach for classification of malignant melanoma and benign skin lesions. Multimedia Tools and Applications pp. 1–18 (2022)
36. Polat, K., Koc, K.O.: Detection of skin diseases from dermoscopy image using the combination of convolutional neural network and one-versus-all. Journal of Artificial Intelligence and Systems 2(1), 80–97 (2020)
37. Gessert, N., Nielsen, M., Shaikh, M., Werner, R., Schlaefer, A.: Skin lesion classification using ensembles of multi-resolution efficientnets with meta data. MethodsX 7, 1–8 (2020)
38. He, X., Wang, Y., Zhao, S., Yao, C.: Deep metric attention learning for skin lesion classification in dermoscopy images. Complex & Intelligent Systems 8(2), 1487–1504 (2022)
39. Abhila, D., Priyankaa, B., Aishwariya, A., Nihal Mathew, S., Suriya Kumar, S., Kumarasamy, K.: Skin lesion characterization with ensembles of machine learning and deep learning models. In: Advances in Energy Technology, pp. 265–278. Springer (2022)
40. Szegedy, C., Vanhoucke, V., Ioffe, S., Shlens, J., Wojna, Z.: Rethinking the inception architecture for computer vision. In: Proceedings of the IEEE conference on computer vision and pattern recognition. pp. 2818–2826 (2016)
41. He, K., Zhang, X., Ren, S., Sun, J.: Deep residual learning for image recognition. In: Proceedings of the IEEE conference on computer vision and pattern recognition. pp. 770–778 (2016)
42. Simonyan, K., Zisserman, A.: Very deep convolutional networks for large-scale image recognition. arXiv preprint arXiv:1409.1556 (2014)
43. Chollet, F.: Xception: Deep learning with depthwise separable convolutions. In: Proceedings of the IEEE conference on computer vision and pattern recognition. pp. 1251–1258 (2017)
44. Howard, A.G., Zhu, M., Chen, B., Kalenichenko, D., Wang, W., Weyand, T., Andreetto, M., Adam, H.: Mobilenets: Efficient convolutional neural networks for mobile vision applications. arXiv preprint arXiv:1704.04861 (2017)
45. Huang, G., Liu, Z., Van Der Maaten, L., Weinberger, K.Q.: Densely connected convolutional networks. In: Proceedings of the IEEE conference on computer vision and pattern recognition. pp. 4700–4708 (2017)